analytical chemistry

Article

pubs.acs.org/ac

Rapid and Highly Sensitive Method for Influenza A (H1N1) Virus Detection

Li-Chen Su,[†,‡] Chung-Ming Chang,[§,∥] Ya-Ling Tseng,[§,∥] Ying-Feng Chang,[‡,⊥] Ying-Chang Li,[†] Yu-Sun Chang,[⊥,¶] and Chien Chou*[,†,‡,#]

[†]Department of Optics and Photonics, National Central University, Taoyuan, Taiwan, 320

[‡]Graduate Institute of Electro-optical Engineering, [§]Research Center for Emerging Viral Infections, [∥]Department of Medical Biotechnology and Laboratory Science, [⊥]Molecular Medicine Research Center, [¶]Graduate Institute of Biomedical Sciences, and [#]Center for Biomedical Engineering, Chang Gung University, Taoyuan, Taiwan, 333

ABSTRACT: In this study, we applied the developed paired surface plasma waves biosensor (PSPWB) in a dual-channel biosensor for rapid and sensitive detection of swine-origin influenza A (H1N1) virus (S-OIV). In conjunction with the amplitude ratio of the signal and the reference channel, the stability of the PSPWB system is significantly improved experimentally. The theoretical limit of detection (LOD) of the dual-channel PSPWB for S-OIV is 30 PFU/mL (PFU, plaque-forming unit), which was calculated from the fitting curve of the surface plasmon resonance signal with a S-OIV clinical isolate concentration in phosphate-buffered saline (PBS) over a range of 18−1.8 × 10^6 PFU/mL. The LOD is 2 orders of magnitude more sensitive than the commercial rapid influenza diagnostic test at worst and an order of magnitude less sensitive than real-time quantitative polymerase chain reaction (PCR) whose LOD for S-OIV in PBS was determined to be 3.5 PFU/mL in this experiment. Furthermore, under in vivo conditions, this experiment demonstrates that the assay successfully measured S-OIV at a concentration of 1.8 × 10^2 PFU/mL in mimic solution, which contained PBS-diluted normal human nasal mucosa. Most importantly, the assay time took less than 20 min. From the results, the dual-channel PSPWB potentially offers great opportunity in developing an alternative PCR-free diagnostic method for rapid, sensitive, and accurate detection of viral pathogens with epidemiological relevance in clinical samples by using an appropriate pathogen-specific antibody.

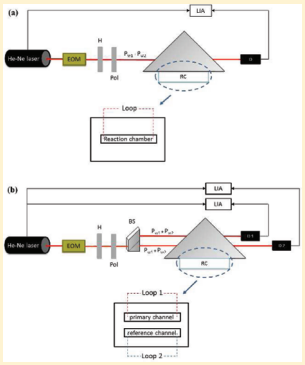

Surface plasmon resonance (SPR) is an optoelectronic phenomenon which involves surface-bound electromagnetic fields, surface plasmon waves (SPWs), penetrating into the dielectric medium approximately 200 nm from the metal/dielectric interface.[1] It belongs to a highly localized electromagnetic field and is very sensitive to changes in the effective refractive index of the dielectric medium near a metal film surface under the attenuated total reflection (ATR) arrangement. Nowadays, SPR sensors have been widely used to investigate biomolecular interactions including antigen−antibody, protein−protein, and DNA−DNA interactions because of the capabilities for rapid, label-free, highly sensitive, and real-time detection.[2−5] However, limits on the detection sensitivity of conventional SPR biosensors render them incapable of detecting small changes in the effective refractive index, particularly in the measurement of biomolecular interactions at ultralow concentrations.[6,7] The conventional SPR biosensor is suitable for detecting larger changes in the effective refractive index caused by cells, bacteria, or viruses.[8−10]

Influenza, an acute respiratory disease caused by the influenza virus, has accounted for major public health concerns with international importance.[11] It can spread worldwide rapidly and cause significant morbidity and mortality, especially in the elderly and children.[12] To control epidemic diseases, there has been wide interest in the development of sensitive, specific, and rapid detection techniques for pandemic influenza virus. Such techniques would help enable diagnosis at an early stage, facilitating the initiation of antiviral treatment as well as for the surveillance of the infection, particularly for those at high risk of influenza-related complications. There are at present two methods used for the diagnosis of influenza A virus infections via clinical samples. The rapid influenza diagnostic test (RIDT) is based on immunochromatographic lateral flow tests and uses monoclonal antibodies directly against the nucleoprotein (NP) of influenza virus.[13] This is currently the best choice for screening samples for the diagnosis of influenza A virus due to its rapid detection ability, simple operation, and low cost. However, RIDT can only distinguish influenza A and influenza B viruses; it is unable to further classify influenza A subtypes. In addition, the limit of detection (LOD) of the RIDT was reported to be in the range of 10^3−10^4 PFU/mL for H1N1 identification and was less accurate (<70%).[14,15] To improve the accuracy and sensitivity of influenza A virus detection, polymerase chain reaction (PCR) based methods such as real-time PCR or RT-PCR were applied. Currently, PCR-based detection methods are the most popular tools for clinical diagnosis of influenza A virus in respiratory specimens. They not only can detect influenza A virus at high sensitivity

Received: October 4, 2011
Accepted: March 7, 2012
Published: March 7, 2012

   dx.doi.org/10.1021/ac3002947 | *Anal. Chem.* 2012, 84, 3914−3920

but also are able to further discriminate among the different subtypes of influenza A virus by using specific primers and probes.[16−18] The accuracy of PCR-based assays is 97% and its LOD is at 0.1−10^2 PFU/mL for influenza A virus.[17−20] However, PCR-based assays have complicated procedures and high costs and demand specially trained technicians.[6,21−23] Furthermore, these methods take a few hours to obtain results compared to just 15 min for RIDT. As a result, PCR-based methods are not ideal candidates in a primary health care setting.[22−24]

Recently, PCR-free detection methods have been proposed and developed in response to the need for rapid and highly sensitive detection methods for clinically relevant viruses; these methods involve biosensing applications.[6,25] Lieber and co-workers used semiconducting nanowires or carbon nanotubes configured as field-effect transistors and were able to detect biological macromolecules.[22,26,27] Weissleder and co-workers developed biocompatible magnetic nanosensors that act as magnetic relaxation switches to detect molecular interactions in the reversible self-assembly of disperse magnetic particles into stable nanoassemblies.[28,29] The SPR technique recently has been intensively investigated and found to be an efficient tool in PCR-free detection.[6,30] Previous research studies on the use of SPR for detecting influenza virus have the advantage of a simple and fast experimental procedure;[31−33] however, many implications for medical health care require as low a detection limit as possible. Therefore, an important goal here is to improve the detection sensitivity of the SPR technique. Previously, a paired surface plasma waves biosensor (PSPWB) was developed based on optical heterodyne technique integrated with amplitude normalization using the reference beam (S polarized waves).[34−36] Experimentally, this system has been demonstrated to meet the requirement of sensitive detection on small molecules or at low concentration in real time.[36] However, the drifts and noise originating from various environmental sources in the detected heterodyne signal of PSPWB limit the detection sensitivity when detecting ultralow concentration under the requirements of label-free and real-time measurement. Hence, a novel dual-channel PSPWB was developed in this study to reduce the noises not only from laser intensity fluctuations but also from environmental variations by using a symmetrical reference channel for a lower detection limit.[37−39] The experimental setup adopted an electro-optic modulator (EOM) to produce optical heterodyne signals instead of an acoustic-optic modulator (AOM) in a Mach−Zehnder interferometer arrangement.[40,41] This configuration contributes to a simpler optical setup with a common-path interferometer and easier alignment. In this study, the dual-channel PSPWB is applied to rapidly detect swine-origin influenza virus (S-OIV), which caused outbreak in April 2009 and is the common subtype of influenza A virus currently circulating in humans. Experimentally, the LOD of the dual-channel PSPWB for S-OIV detection is estimated to be 30 PFU/mL, which is an order of magnitude worse than that by quantitative PCR (qPCR) at 3.5 PFU/mL. Additionally, the assay time of dual-channel PSPWB is similar to that of RIDT. It is important to note that this work potentially offers great opportunity to develop an alternative PCR-free method able to detect not only S-OIV but also other viral pathogens by incorporating an appropriate pathogen-specific antibody.

EXPERIMENTAL SECTION

Materials. The bare silver/gold chips used in this study were produced by the Thin Film Technology Center at the National Central University (Taoyuan, Taiwan). The amine coupling kit containing 1-ethyl-3-(3-dimethylaminopropyl)-carbodiimide hydrochloride (EDC), *N*-hydroxysuccinimide (NHS), and 1.0 M ethanolamine-HCl, pH 8.5 (ETH) was purchased from Biacore, Inc. (Uppsala, Sweden). $C_{25}H_{44}O_6S_2$ and $C_{33}H_{58}O_{11}S_2$ were obtained from SensoPath Technologies (Bozeman, MT), while anti-(S-OIV) H1 antibody (a-H1) was purchased from ProSci (Poway, CA). Minimum Essential Medium (MEM) was purchased from Invitrogen (Carlsbad, CA). All chemicals were used without further purification. A commercial Flu A/B rapid test kit was obtained from Formosa Biomedical Technology Corp. (Taipei, Taiwan). Influenza virus strain, S-OIV, was obtained from Chang Gung Memorial Hospital, Lin-Kou, Taiwan. The viruses were isolated from a throat swab of a patient by Madin−Darby canine kidney (MDCK) cell lines and were confirmed by viral culture and molecular analysis with CDC protocol (CDC Protocol of realtime RTPCR for influenza A (H1N1) April 28, 2009 Revision 2). The original S-OIV virus titer was 1.8×10^6 PFU/mL in the culture medium (MEM).

Rapid Influenza Diagnostic Test for Detection of S-OIV. The commercial Flu A/B rapid test kit (Lot. MS199R1, Formosa Biomedical, Taiwan) was used to perform virus detection according to the manufacturer's protocol. S-OIVs solution (140 μL) of each concentration was mixed with lysis buffer and reactive antibody-conjugated horseradish peroxidase (HRP) in one tube and then the testing strip coated with specific Flu A/B nucleoprotein monoclonal antibody was inserted into the tube. Positive or negative influenza diagnostic result was obtained from different significant bands that appeared on the strip paper after 15 min of incubation.

Real-Time Quantitative RT-PCR for Detection of S-OIV. With the LightCycler 480 system and RNA Master Hydrolysis Probes System (ROCHE), one-step qPCR targeting the conserved matrix gene segment with a specific probe for influenza detection was performed to detect the presence of S-OIV in a serial dilution sample. Reactions were carried out in a total volume of 20 μL of 1X PCR mixture containing 5 μL of testing sample, oligonucleotides FluA-M52C (5′-CTT CTA ACC GAG GTC GAA ACG-3′) and FluA-M253R (5′-AGG GCA TTT TGG ACA AAK CGT CTA-3′) at 0.5 μM each,[42] and the specific M probe: (5′-(Fam) CCT CAA AGC CGA GAT CGC GCA (Tamra)-3′) of 0.2 μM. PCR reaction conditions were as follows: 63 °C for 10 min, 95 °C for 30 s, and 45 cycles of amplification: 95 °C for 15 s, 55 °C for 10 s, and 72 °C for 20 s with the final cooling at 40 °C for 10 s. All serially diluted samples were run in duplicate with the influenza virus A/Hong Kong/427/98 as a positive control.

Preparation of SPR Chip. The SPR chip used in this study was a BK7 glass slide coated with a laminated Ag/Au (37/8 nm) metal layer. A mixed self-assembled monolayer (SAM) of dithiols consisting of 90% $C_{25}H_{44}O_6S_2$ and 10% $C_{33}H_{58}O_{11}S_2$ used as a diluent at a mixing ratio of 1:9 was assembled at the Ag/Au substrates, generating a binding matrix optimized for the formation of a capture antibody monolayer via the amine-coupling protocol. The capture antibody was covalently immobilized to the SPR sensor chip according to the amine-coupling protocol, performed as follows:

dx.doi.org/10.1021/ac3002947 | *Anal. Chem.* 2012, 84, 3914−3920

1. The modified chip was activated by immersing it in the mixed solutions, which included 0.4 M EDC and 0.1 M NHS, for about 10 min.

2. The capture antibody, at a concentration of 40 μg/mL prepared in immobilization buffer, was immobilized via the reaction of primary amine groups or other nucleophilic groups, and then incubated with the sensor chip surface. This process was carried out for about 30 min.

3. ETH was injected to block the active sites of nonreacted surface. This process was carried out for 7 min.

Measurement of S-OIV Using Single-Channel and Dual-Channel PSPWBs. The UV-irradiated target S-OIV in PBS solution was injected into the reaction chamber to interact with the immobilized capture antibody on the SPR sensor chip to form the "capture antibody/S-OIV" complex. In addition, we utilized the S-OIV isolate diluted in normal human nasal mucosa (called mimic solution) to mimic in vivo isolation of influenza virus from the upper human respiratory tract. In these experiments, the control group was tenfold diluted blank culture medium that did not contain S-OIV.

Figure 1 illustrates the optical setups of single-channel and dual-channel PSPWB. The laser beam from a frequency-

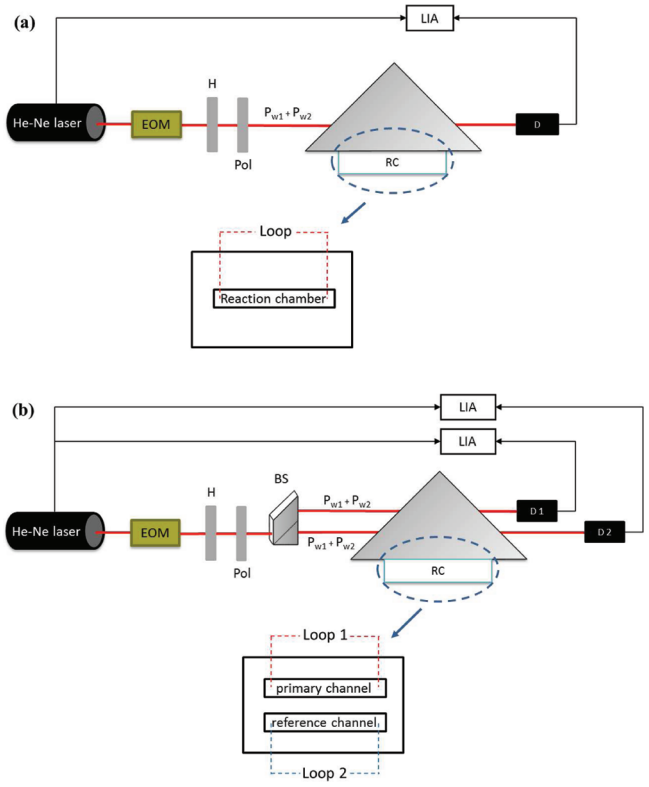

Figure 1. Experimental setup of PSPWB: (a) single channel; (b) dual channel. EOM, electro-optic modulator; H, half wave plate; Pol, polarizer; BS, beam splitter; RC, reaction chamber; D, photo detector; LIA, lock-in amplifier.

stabilized and linearly polarized He−Ne laser with wavelength of 632.8 nm integrated with an EOM that is driven at frequency ω. Then the beam passes through a half wave plate and a polarizer sequentially to produce two highly correlated P polarized waves (TM wave, $P_{\omega 1}$ and $P_{\omega 2}$) at different frequencies. For single-channel PSPWB, the P polarized light was directly incident to the SPR device and detected by a photo detector. Finally, a lock-in amplifier is introduced to measure the amplitude of P heterodyne signal. In dual-channel PSPWB, the P polarized light is split into two parallel beams by undergoing a lateral displacement beamsplitter, and was subsequently incident to a dual-channel SPR device. Two lock-in amplifiers are used for simultaneously measuring the amplitudes of P heterodyne signals from the reference channel and signal channel respectively for S-OIV detection.

RESULTS AND DISCUSSION

System Stability of the Single-Channel and Dual-Channel PSPWB. In this study, the single-channel PSPWB was extended into a dual-channel biosensor. The stabilities of these two systems were tested simultaneously by tridistilled water when the incident angle of the laser beam was near the SPR angle and were expressed as percentage error of the system, which is calculated by

$$\text{percentage error} = \frac{R_{\text{each point}} - R_{\text{mean}}}{R_{\text{mean}}} \times 100\%$$

where $R = ((S_p - S_r)/(S_r))$ is defined as response; S_p and S_r are described as the heterodyne signals of the reflected P polarized waves from signal (primary) channel and reference channel, respectively, in the dual-channel PSPWB. While in the single-channel PSPWB, R is the heterodyne signal of the reflected P polarized waves from the reaction chamber. The results are shown in Figure 2 in which the relative standard deviations

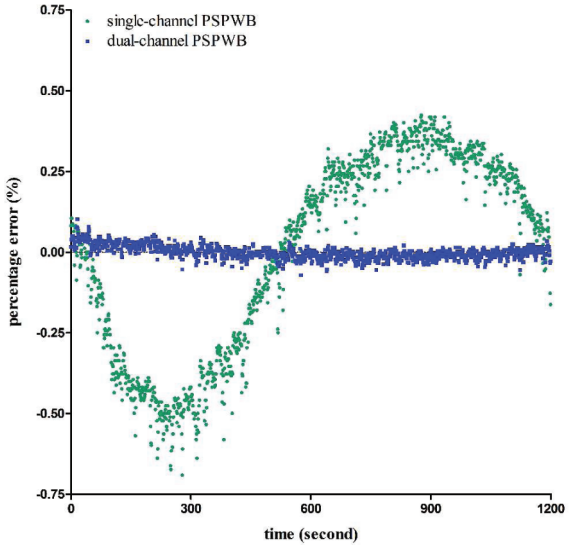

Figure 2. Stabilities of single-channel and dual-channel PSPWBs by testing tridistilled water spanning 20 min. The RSDs of system stabilities were 0.31% and 0.02% for the single-channel and dual-channel PSPWBs, respectively, in this experiment.

(RSD) of system stabilities spanning 20 min were 0.31% and 0.02% for the single-channel PSPWB and the dual-channel PSPWB, respectively, in this experiment. It is obvious that the instability of the single-channel PSPWB system was reduced significantly by using the amplitude ratio method with the reference channel.

Performance of the Single-Channel and Dual-Channel PSPWBs on Detecting S-OIV. The SPR sensor chip was prepared using the method described above, and the original concentration of the UV-irradiated S-OIV culture supernatant before PBS dilution was 1.8×10^6 PFU/mL. After a-H1 was

dx.doi.org/10.1021/ac3002947 | Anal. Chem. 2012, 84, 3914−3920

immobilized onto the SPR sensor chip, tenfold serial dilutions of S-OIV culture supernatant in 1 mL volume each, that is, 18 PFU/mL, 1.8×10^2 PFU/mL, 1.8×10^3 PFU/mL, 1.8×10^4 PFU/mL, 1.8×10^5 PFU/mL, and 1.8×10^6 PFU/mL, were prepared in PBS solution separately and then were injected into the reaction chamber to interact with the immobilized a-H1. Meanwhile, zero concentration is treated as tenfold diluted blank culture medium, which is the control group. The real-time interaction was measured by the single-channel and dual-channel PSPWB systems, both represented in Figure 3. And

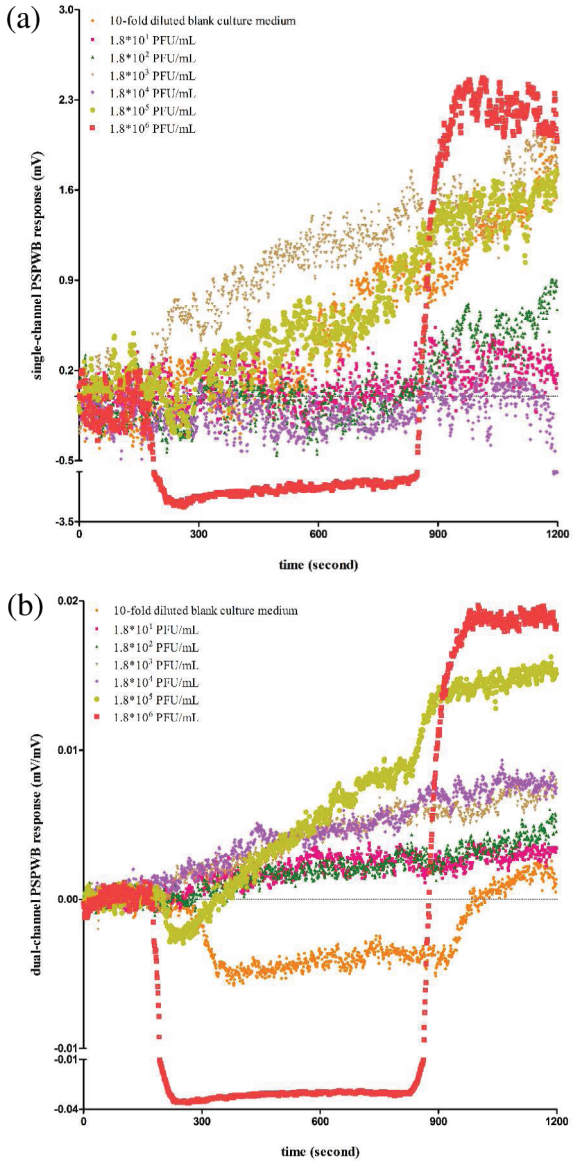

Figure 3. Binding processes of a-H1 interaction with different concentrations of S-OIV over the range 18−1.8×10^6 PFU/mL while zero concentration is treated as tenfold diluted blank culture medium which is the control group: (a) single-channel PSPWB; (b) dual-channel PSPWB.

then the SPR signal was obtained by subtracting the background level from the average of the response over the last 100 data points in the experiment. Therefore, the unit of the SPR signal is expressed as ((mV)/(mV)), usually named arbitrary unit (a.u.). For the dual-channel PSPWB, the correlation between the SPR signal and the concentration of the S-OIV clinical isolate over the range of 18−1.8×10^6 PFU/mL were shown in Figure 4. The results were analyzed using a

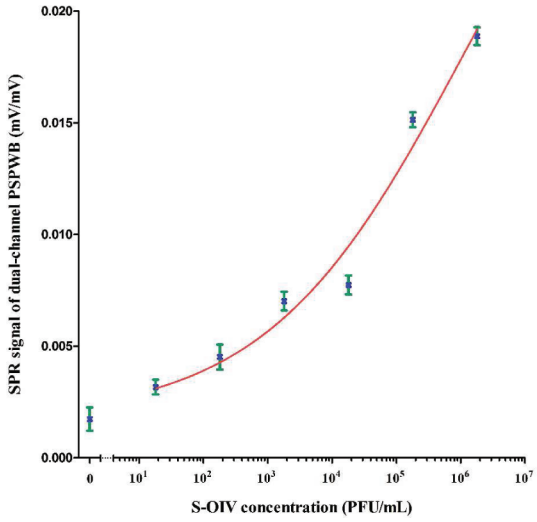

Figure 4. Correlation (R^2 = 0.9735) between the SPR signal and the concentration of S-OIV over the range 18−1.8×10^6 PFU/mL. The error bar indicates 1 SD in each measurement. Zero concentration is treated as tenfold diluted blank culture medium, which is the control group.

sigmoidal dose−response curve with variable slope, also called a four-parameter logistic equation, found in GraphPad Prism software; the correlation coefficient (R^2) is 0.9735 and the error bar indicates 1 SD in each measurement. Theoretical LOD of dual-channel PSPWB was calculated to be 30 PFU/mL from both experimental data and the fitting curve for this experimental design. However, for the single-channel PSPWB, there is no correlation between the SPR signal and the concentration of the S-OIV clinical isolate in the range of 18−1.8×10^6 PFU/mL.

Detection of S-OIV in Mimic Solution Using the Dual-Channel PSPWB. To mimic the human respiratory tract condition in vivo, we conducted studies with diluted S-OIV isolate in mimic solution. The results presented in Figure 5 demonstrate that a 10^4-fold dilution of S-OIV culture supernatant (1.8×10^2 PFU/mL) in mimic solution was successfully detected by the dual-channel PSPWB because the signal exceeded 3 times the standard deviation from tenfold diluted blank culture medium, which corresponded to the medium-only control.

Detection of S-OIV by Rapid Influenza Diagnostic Test in PBS and in Mimic Solution. The commercial RIDT, Flu A/B rapid test, is currently used for fast clinical diagnosis of influenza A and B virus infection in some hospitals. We also used this assay to detect a clinical S-OIV isolate diluted in PBS and in mimic solution. Table 1 shows that the LOD of the Flu A/B rapid test was 100-fold dilution (1.8×10^4 PFU/mL) of the original S-OIVs in PBS and 1.8×10^5 PFU/mL in mimic solution in this assay.

Detection of S-OIV by Real-Time Quantitative RT-PCR in PBS and in Mimic Solution. Serial tenfold dilutions of S-OIV (1 to 10^7-fold dilution of the original S-OIV isolate) were made to carry out detection sensitivity test of qPCR. Then, the threshold cycle (Ct) values of the serial dilution were plotted versus the concentration of the S-OIV clinical isolate as shown in Figure 6, where the Ct value is defined as the cycle number

dx.doi.org/10.1021/ac3002947 | Anal. Chem. 2012, 84, 3914−3920

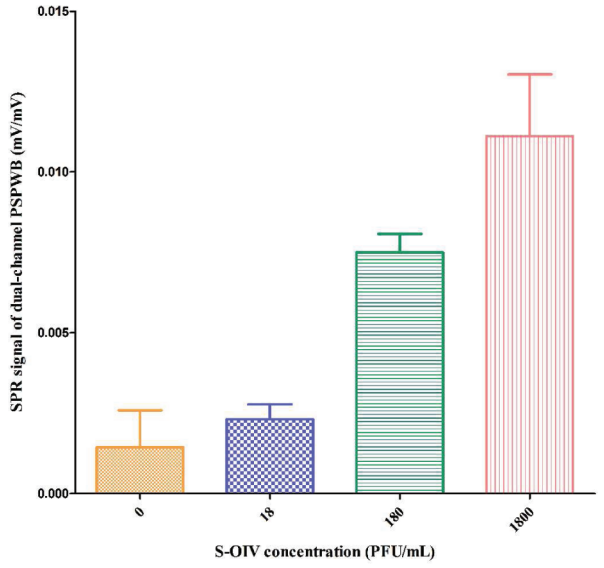

Figure 5. SPR signals of binding between a-H1 and S-OIV clinical isolates at different concentrations in mimic solution. Zero concentration is treated as tenfold diluted blank culture medium, which is the control group.

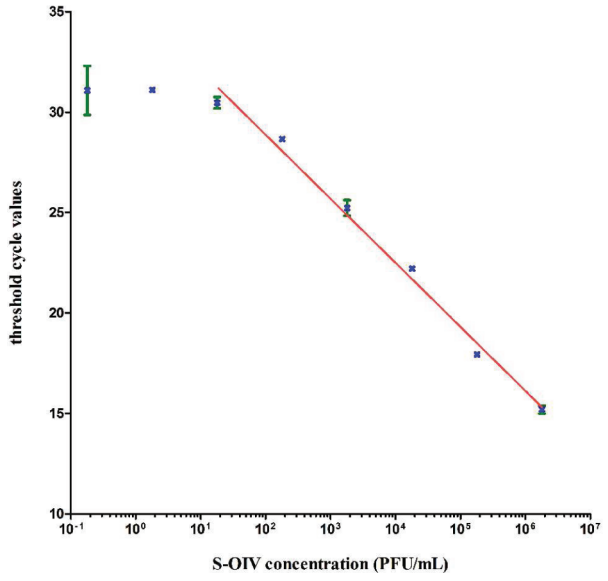

Figure 6. Threshold cycle (Ct) values of the serial dilutions are plotted against the logarithm of the concentration of the S-OIV clinical isolate in PBS. Linear standard curve (R^2 = 0.9905) obtained from dilution series of S-OIV in a range from 18 to 1.8 × 10^6 PFU/mL with two replications per quantity.

Table 1. Experimental Results of S-OIV in PBS in Different Methods, Including Dual-Channel PSPWB, qPCR, and RIDT[a]

target virus	S-OIV (H1N1)							
detection method	dual-channel PSPWB (directly detection of viral particles)							
virus concentration (PFU/mL)	1.8×10^6	1.8×10^5	1.8×10^4	1.8×10^3	1.8×10^2	18	1.8	0.18
testing result	+	+	+	+	+	+/-		
detection method	qPCR (viral nucleic acid amplification needed)							
virus concentration (PFU/mL)	1.8×10^6	1.8×10^5	1.8×10^4	1.8×10^3	1.8×10^2	18	1.8	0.18
testing result	+	+	+	+	+	+	+/-	+/-
detection method	commercial rapid influenza diagnostic test (RIDT)							
virus concentration (PFU/mL)	1.8×10^6	1.8×10^5	1.8×10^4	1.8×10^3	1.8×10^2	18	1.8	0.18
testing result	+	+	+	-	-			

[a]PFU, plaque-forming unit; "+", positive; "−", negative; "±", virus was detectable, but lower than the theoretical LOD.

Table 2. Comparison of Three Assays for S-OIV Detection, Including Time Cost, Detection Target, and Limit of Detection

	qPCR	dual-channel PSPWB	RIDT
time cost	within 3 hrs	~ 20 mins	~ 15 mins
detection target	nucleic acid	hemagglutinin	nucleoprotein
limit of detection (PBS)	~ 3.5 PFU/mL (calculated)	~ 30 PFU/mL (calculated)	1.8×10^4 PFU/mL
detectable concentration (mimic solution)	1.8×10^3 PFU/mL	1.8×10^2 PFU/mL	1.8×10^5 PFU/mL

at which the fluorescence generated within a reaction crosses the threshold. Meanwhile, a linear relationship between the Ct value and the concentration of the S-OIV clinical isolate over the range of 18−1.8 × 10^6 PFU/mL (1 to 10^5-fold dilution) was obtained; the correlation coefficient (R^2) is 0.9905. The viral concentrations of 0.18 and 1.8 PFU/mL were detectable but not in the linear range. Therefore, the theoretical LOD of qPCR is calculated at 3.5 PFU/mL in PBS solution according to the International Union of Pure and Applied Chemistry (IUPAC) criteria.[20] In addition, the detectable concentration of S-OIV culture supernatant in mimic solution was 1.8 × 10^3 PFU/mL experimentally.

Tables 1 and 2 show a comparison between the different assays for the detection of S-OIV in this experiment. It is obvious that qPCR is still the most sensitive method for S-OIV detection in PBS solution. However, typical RT-PCR assays take about 1−2 h for thermocycling, a significant portion of cycling time spent for heating and cooling. Thus, there has been growing interest in the reduction of PCR cycling times.[43] Although Yoon et al. presented a novel method to significantly reduce the time for PCR thermocycling to achieve 30-cycle less than 20 min by employing wire-guide droplet microfluidics, the time for RNA extraction and PCR analysis still needs at least 90 min. But with detection of S-OIV in mimic solution containing normal human nasal mucosa, the detectable concentration by qPCR assay decreased by 2 orders of magnitude. It might result from the presence of inhibitors to reduce or block PCR amplification.[44,45] In contrast, for dual-channel PSPWB, the detectable concentration in mimic solution was just an order of magnitude less than that in PBS solution; this situation also occurred when commercial RIDT was used. It is interesting that these two assays were based on protein detection of S-OIV such as hemagglutinin or nucleoprotein, respectively. This implies that the problem of inhibitor interference in sample for qPCR is more serious than nonspecific binding for protein detection. Besides, the dual-channel PSPWB offers a reduced assay time for pathogen detection comparable with commercial RIDT. In addition, the assay is performed immediately within 20 min or less after specimen collection as opposed to several hours by PCR-based methods.

dx.doi.org/10.1021/ac3002947 | Anal. Chem. 2012, 84, 3914−3920

In this study, the dual-channel PSPWB used an EOM to produce optical heterodyne signals in a common-path optical setup instead of AOM in the Mach−Zehnder interferometer arrangement and consequently showed simpler and better alignment than conventional PSPWB. In addition, the combination of a reference channel improved the stability of PSPWB by an order of magnitude better experimentally due to the reduction of laser intensity fluctuations and environmental disturbances, such as inject noise in the reaction chamber in the SPR device during measurement.[46,47] These factors contributed a higher signal-to-noise ratio, which has been shown to enhance the detection sensitivity of SPR sensors.[48] The advantages of the dual-channel PSPWB with fast and highly sensitive abilities can be the crucial factors in identifying epidemiologically relevant organisms, such as S-OIV, especially when rapid diagnosis may prevent the spread of infectious agents before they become pandemic.[23,49]

■ CONCLUSIONS

We proposed a novel S-OIV diagnostic platform, the dual-channel PSPWB integrating an optical common-path heterodyne technique and dual-channel SPR sensing device, for highly sensitive and rapid detection of viruses based on immunoassay technology without the need for PCR amplification. These results reveal that the dual-channel PSPWB using specific antibodies against HA proteins of S-OIV can obtain higher sensitivity compared to conventional RIDTs. Moreover, the theoretical LOD of dual-channel PSPWB for S-OIV detection in PBS is 30 PFU/mL, which is an order of magnitude worse than qPCR at 3.5 PFU/mL of S-OIV in this experiment. Meanwhile, S-OIV culture supernatant of 1.8×10^2 PFU/mL in mimic solution was also detected successfully, whereas the assay time was reduced to 20 min. These results show that the dual-channel PSPWB potentially becomes a PCR-free biosensor for the rapid and accurate diagnosis of S-OIV infection or other viral pathogens via an appropriate pathogen-specific antibody in the near future.

■ AUTHOR INFORMATION

Corresponding Author

*Telephone: 886-3-2118800, ext. 3677. Fax: 886-3-2118507. E-mail: cchou@mail.cgu.edu.tw.

Notes

The authors declare no competing financial interest.

■ ACKNOWLEDGMENTS

This research was supported by the National Science Council of Taiwan through research grants: NSC 98-2221-E-182-063-MY3, NSC 98-2221-E-182-064-MY3, and NSC 98-2321-B-182-001. Partial support from the Ministry of Education, aiming for the Top University Plan (EMRPD190041), and the support of the Healthy Aging Research Center of Chang Gung University is also appreciated. Li-Chen Su and Chung-Ming Chang contributed equally to this work.

■ REFERENCES

(1) Yu, F.; Yao, D.; Knoll, W. *Anal. Chem.* **2003**, *75*, 2610−2617.
(2) Homola, J. *Chem. Rev.* **2008**, *108*, 462−493.
(3) Wong, C. L.; Ho, H. P.; Suen, Y. K.; Kong, S. K.; Chen, Q. L.; Yuan, W.; Wu, S. Y. *Biosens. Bioelectron.* **2008**, *24*, 606−612.
(4) Arima, Y.; Toda, M.; Iwata, H. *Adv. Drug Delivery Rev.* **2011**, *63*, 988−999.
(5) Khan, S. H.; Farkas, K.; Kumar, R.; Ling, J. *Anal. Biochem.* **2012**, *421*, 385−390.
(6) Kim, S. A.; Byun, K. M.; Kim, K.; Jang, S. M.; Ma, K.; Oh, Y.; Kim, D.; Kim, S. G.; Shuler, M. L.; Kim, S. J. *Nanotechnology* **2010**, *21*, 355503.
(7) He, L.; Musick, M. D.; Nicewarner, S. R.; Salinas, F. G.; Benkovic, S. J.; Natan, M. J; Keating, C. D. *J. Am. Chem. Soc.* **2000**, *122*, 9071−9077.
(8) Chiang, Y.-L.; Lin, C.-H.; Yen, M.-Y.; Su, Y.-D.; Chen, S.-J.; Chen, H.-f. *Biosens. Bioelectron.* **2009**, *24*, 1905−1910.
(9) Nilsson, C. E.; Abbas, S.; Bennemo, M.; Larsson, A.; Hämäläinen, M. D.; Frostell-Karlsson, Å. *Vaccine* **2010**, *28*, 759−766.
(10) Caygill, R. L.; Blair, G. E.; Millner, P. A. *Anal. Chim. Acta* **2010**, *681*, 8−15.
(11) Castillo-Salgado, C. *Epidemiol. Rev.* **2010**, *32*, 93−109.
(12) Ghebremedhin, B.; Engelmann, I.; Konig, W.; Konig, B. *J. Med. Microbiol.* **2009**, *58*, 365−370.
(13) Taylor, J.; McPhie, K.; Druce, J.; Birch, C.; Dwyer, D. E. *J. Med. Virol.* **2009**, *81*, 1918−1922.
(14) Kwon, D.; Shin, K.; Kwon, M.; Oh, H.-B.; Kang, C.; Lee, J.-Y. *J. Clin. Microbiol.* **2011**, *49*, 437−438.
(15) Tsao, K.-C.; Kuo, Y.-B.; Huang, C.-G.; Chau, S.-W.; Chan, E.-C. *J. Virol. Methods* **2011**, *173*, 387−389.
(16) Wenzel, J. J.; Walch, H.; Bollwein, M.; Niller, H. H.; Ankenbauer, W.; Mauritz, R.; Höltke, H.-J.; Zepeda, H. M.; Wolf, H.; Jilg, W.; Reischl, U. *Clin. Chem.* **2009**, *55*, 2218−2222.
(17) Bose, M. E.; Beck, E. T.; Ledeboer, N.; Kehl, S. C.; Jurgens, L. A.; Patitucci, T.; Witt, L.; LaGue, E.; Darga, P.; He, J.; Fan, J.; Kumar, S.; Henrickson, K. J. *J. Clin. Microbiol.* **2009**, *47*, 2779−2786.
(18) He, J.; Bose, M. E.; Beck, E. T.; Fan, J.; Tiwari, S.; Metallo, J.; Jurgens, L. A.; Kehl, S. C.; Ledeboer, N.; Kumar, S.; Weisburg, W.; Henrickson, K. J. *J. Clin. Microbiol.* **2009**, *47*, 2772−2778.
(19) Hamelin, M.-E.; Baz, M.; Abed, Y.; Couture, C.; Joubert, P.; Beaulieu, E.; Bellerose, N.; Plante, M.; Mallett, C.; Schumer, G.; Kobinger, G. P.; Boivin, G. *PLoS Pathog.* **2010**, *6*, e1001015.
(20) Furuse, Y.; Odagiri, T.; Okada, T.; Khandaker, I.; Shimabukuro, K.; Sawayama, R.; Suzuki, A.; Oshitani, H. *J. Virol. Methods* **2010**, *168*, 94−97.
(21) Amano, Y.; Cheng, Q. *Anal. Bioanal. Chem.* **2005**, *381*, 156−164.
(22) Patolsky, F.; Zheng, G.; Hayden, O.; Lakadamyali, M.; Zhuang, X.; Lieber, C. M. *Proc. Natl. Acad. Sci. U.S.A.* **2004**, *101*, 14017−14022.
(23) Chan, K. H.; Lai, S. T.; Poon, L. L. M.; Guan, Y.; Yuen, K. Y.; Peiris, J. S. M. *J. Clin. Virol.* **2009**, *45*, 205−207.
(24) Cao, C.; Dhumpa, R.; Bang, D. D.; Ghavifekr, Z.; Høgberg, J.; Wolff, A. *Analyst* **2010**, *135*, 337−342.
(25) Driskell, J. D.; Jones, C. A.; Tompkins, S. M.; Tripp, R. A. *Analyst* **2011**, *136*, 3083−3090.
(26) Cui, Y.; Wei, Q.; Park, H.; Lieber, C. M. *Science* **2001**, *293*, 1289−1292.
(27) Zheng, G.; Patolsky, F.; Cui, Y.; Wang, W. U.; Lieber, C. M. *Nat. Biotechnol.* **2005**, *23*, 1294−1301.
(28) Perez, J. M.; Josephson, L.; O'Loughlin, T.; Högemann, D.; Weissleder, R. *Nat. Biotechnol.* **2002**, *20*, 816−820.
(29) Perez, J. M.; Simeone, F. J.; Saeki, Y.; Josephson, L.; Weissleder, R. *J. Am. Chem. Soc.* **2003**, *125*, 10192−10193.
(30) D'Agataa, R.; Corradini, R.; Ferretti, C.; Zanoli, L.; Gatti, M.; Marchelli, R.; Spoto, G. *Biosens. Bioelectron.* **2010**, *25*, 2095−2100.
(31) Critchley, P.; Dimmock, N. J. *Bioorg. Med. Chem.* **2004**, *12*, 2773−2780.
(32) Mandenius, C.-F.; Wang, R.; Alden, A.; Bergstrom, G.; Thebault, S.; Lutsch, C.; Ohlson, S. *Anal. Chim. Acta* **2008**, *623*, 66−75.
(33) Hardy, S. A.; Dimmock, N. J. *J. Virol.* **2003**, *77*, 1649−1652.
(34) Kuo, W.-C.; Chou, C.; Wu, H.-T. *Opt. Lett.* **2003**, *28*, 1329−1331.
(35) Chou, C.; Wu, H.-T.; Huang, Y.-C.; Kuo, W.-C.; Chen, Y.-L. *Opt. Express* **2006**, *14*, 4307−4315.

(36) Su, L.-C.; Chen, R.-C.; Li, Y.-C.; Chang, Y.-F.; Lee, Y.-J.; Lee, C.-C.; Chou, C. *Anal. Chem.* **2010**, *82*, 3714−3718.
(37) Nenninger, G. G.; Clendenning, J. B.; Furlong, C. E.; Yee, S. S. *Sens. Actuators, B* **1998**, *51*, 38−45.
(38) Naimushin, A. N.; Soelberg, S. D.; Nguyen, D. K.; Dunlap, L.; Bartholomew, D.; Elkind, J.; Melendez, J.; Furlong, C. E. *Biosens. Bioelectron.* **2002**, *17*, 573−584.
(39) Peng, W.; Banerji, S.; Kim, Y.-C.; Booksh, K. S. *Opt. Lett.* **2005**, *30*, 2988−2990.
(40) Chiu, M.-H.; Lee, J.-Y.; Su, D.-C. *Appl. Opt.* **1997**, *36*, 2936−2939.
(41) Yu, C.-J.; Lin, C.-E.; Teng, H.-K.; Tsai, C.-C.; Chou, C. *Opt. Commun.* **2009**, *282*, 1516−1520.
(42) Fouchier, R. A. M.; Bestebroer, T. M.; Herfst, S.; Van Der Kemp, L.; Rimmelzwaan, G. F.; Osterhaus, A. D. *J. Clin. Microbiol.* **2000**, *38*, 4096−4101.
(43) You, D. J.; Tran, P. L.; Kwon, H.-J.; Patel, D.; Yoon, J.-Y. *Faraday Discuss.* **2011**, *149*, 159−170.
(44) Das, A.; Spackman, E.; Pantin-Jackwood, M. J.; Suarez, D. L. *J. Vet. Diagn. Invest.* **2009**, *21*, 771−778.
(45) Poddar, S. K.; Sawyer, M. H.; Connor, J. D. *J. Med. Microbiol.* **1998**, *47*, 1131−1135.
(46) Myszka, D. G. *J. Mol. Recognition* **1999**, *12*, 279−284.
(47) Nizamov, S.; Mirsky, V. M. *Biosens. Bioelectron.* **2011**, *28*, 263−269.
(48) Piliarik, M.; Homola, J. *Opt. Express* **2009**, *17*, 16505−16517.
(49) Cunha, B. A.; Thekkel, V.; Cohan, C. *Infect. Control. Hosp. Epidemiol.* **2010**, *31*, 102−104.